

Stable isotope variations in a coral (*Favia speciosa*) from the Gulf of Kutch during 1948–1989 A.D.: Environmental implications

S CHAKRABORTY and R RAMESH

Physical Research Laboratory, Navrangpura, Ahmedabad 380 009, India
e-mail: r.ramesh@prl.ernet.in

The stable isotopic analyses ($\delta^{18}\text{O}$ and $\delta^{13}\text{C}$) of a coral *Favia speciosa* spanning forty two years (1948–89 A.D.), collected from the Pirotan island (22.6°N, 70°E) in the Gulf of Kutch have been carried out to assess its potential for retrieving past environmental changes in this region. It is seen that the summer (minima) $\delta^{18}\text{O}$ variations in the coral CaCO_3 are negatively correlated with seasonal (summer) monsoon rainfall in the adjoining region of Kutch and Saurashtra and a qualitative reconstruction of historical rainfall variations in this region can be obtained by analyzing the $\delta^{18}\text{O}$ in this species of coral. The observed mean seasonal range of $\delta^{18}\text{O}$ variations is $0.34 \pm 0.17\text{‰}$ ($n = 42$), whereas the expected range calculated (from available SST and measured $\delta^{18}\text{O}$ of sea water) is $\sim 1.1 \pm 0.15\text{‰}$. The difference is due to the coarse resolution of sampling, which can be corrected. The seasonal range in $\delta^{13}\text{C}$ is $\sim 1\text{‰}$ and is explained by changes in: a) the light intensity related to the cloudiness during monsoons and b) phytoplankton productivity.

1. Introduction

To understand various climatic phenomena and their interlinkages it is essential to have a comprehensive data base both from regular meteorological observations and natural proxy records, which extend the data base back in time. In this context, isotopic analysis of corals is useful for monitoring historical changes of climate and physical properties of the surface ocean. The oxygen isotopic variations in coral skeletons have been shown to be useful for monitoring seasonal and annual temperature variations including El Niño in different oceanic regions (Weber and Woodhead 1972; Fairbanks and Dodge 1979; Dunbar and Wellington 1981; Druffel 1985; Charles *et al* 1997). Shen and Sanford (1990), and Cole and Fairbanks (1990) found that the $\delta^{18}\text{O}$ of corals from Tarawa Atoll (Republic of Kiribati) is also inversely related to local precipitation. Aharon (1991) investigated the isotopic records of corals, giant clams and calcareous algae of Great Palm Island and found that the coral $\delta^{18}\text{O}$ was con-

trolled both by temperature and salinity, modulated by rainfall. We (Chakraborty and Ramesh 1992; 1993; 1997) have shown that the seasonal amplitude in $\delta^{18}\text{O}$ of corals from Lakshadweep islands (Arabian Sea) reflects the monsoon induced sea surface cooling of 4°C.

The most characteristic feature of the Arabian Sea is the occurrence of south west (SW) summer monsoon associated with intense winds resulting in a large scale surface ocean circulation (Shetye *et al* 1990) and rainfall over the Indian subcontinent. During winter, the wind direction reverses leading to changes in the surface ocean currents. The SW monsoon causes upwelling of cool, nutrient rich water in several areas like the Somali basin and the west coast of India. In this paper we report $\delta^{18}\text{O}$ and $\delta^{13}\text{C}$ data of a coral collected from the Pirotan island (figure 1), Gulf of Kutch (northern Arabian Sea) and examine their utility as proxy records of SST and monsoon rainfall. Gulf of Kutch (figure 1, mean water depth ~ 30 m) is a shallow well-mixed region where the seasonal SST variations (figure 2) seem to be mainly controlled by

Keywords. Climate; monsoon; SST; stable isotopes; corals; Gulf of Kutch.

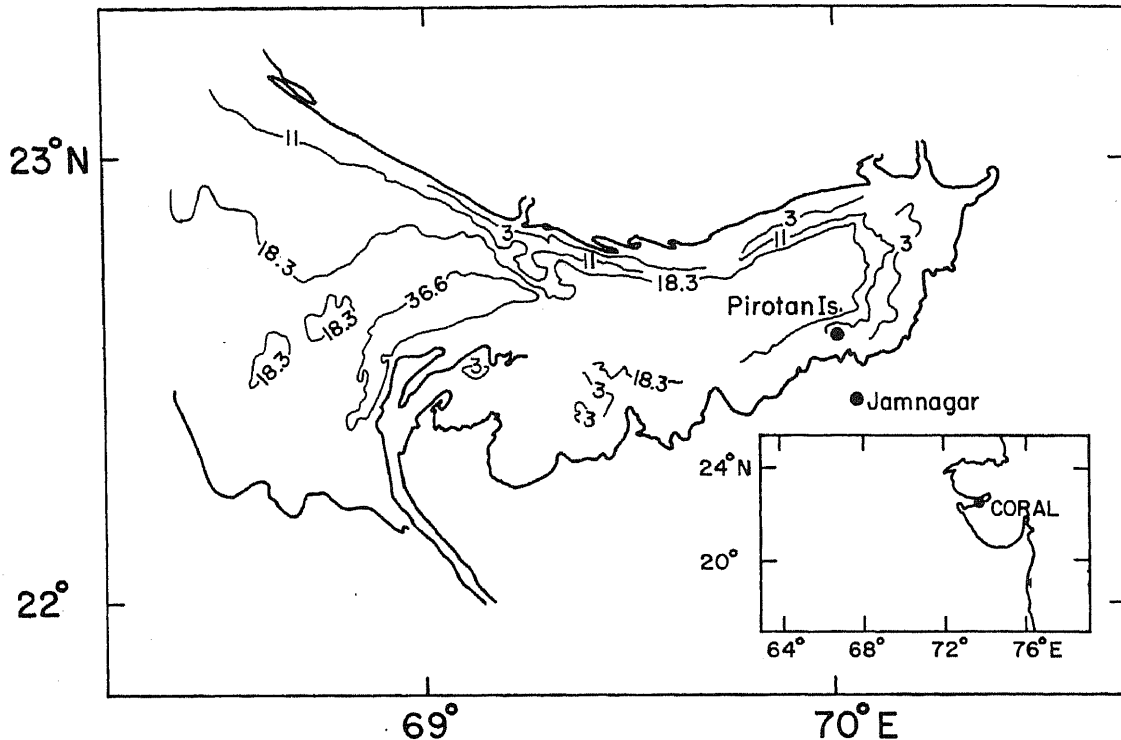


Figure 1. Sample location in the Gulf of Kutch. Contours show water depth in meters.

summer solar heating and winter cooling. Nevertheless, the cloud cover during the SW monsoon reduces the SST by about 2°C in the Gulf.

2. Methods

A live coral head, *Favia speciosa* was collected in June 1990 off the coast of Pirotan island situated in the Gulf of Kutch at a water depth of ~ 1 metre during low tide. The sample was washed with fresh water, dried and cut into a vertical section (~ 1 cm thick) along the growth axis. The annual bands (consisting of light and dark rings) were photographed using the standard X-ray technique (Wellington and Glynn 1983) and counted to determine the age, assuming that the latest band, which had only developed the light part, corresponds to 1990 (this band, however, was not analyzed for stable isotopes, as it was only partially formed and contained considerable organic matter). The annual band widths (i.e., growth rates) were measured from the X-ray positive using a hand lens fitted with a scale correct to 0.1 mm. Milligram quantities of calcium carbonate powder were removed from a radial strip by careful filing, taking 2 to 8 samples per annual band. The extracted powder was roasted under vacuum at 350°C for an hour to remove organic matter. Isotopic measurements were made using a VG 903 mass-spectrometer following standard techniques (Chakraborty and Ramesh 1997) and the results reported in δ notation with respect to PDB with a precision of 0.07‰ for both $\delta^{18}\text{O}$ and $\delta^{13}\text{C}$.

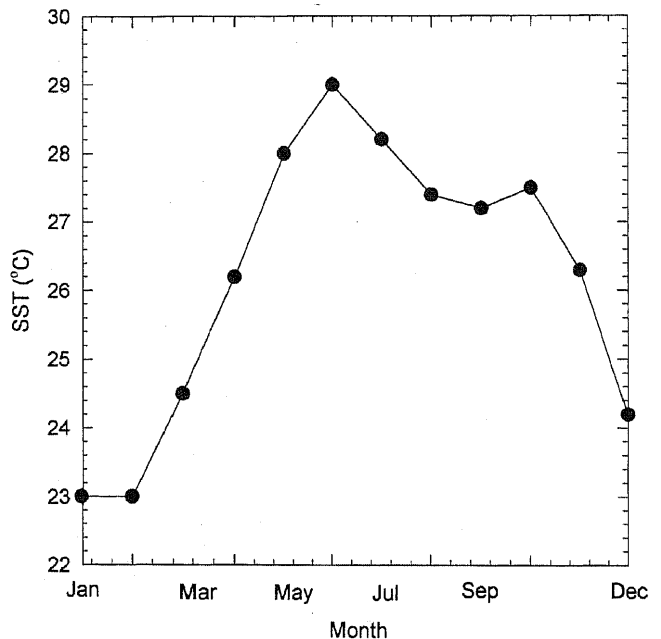


Figure 2. Seasonal sea surface temperature variations near the sample location (Sadler *et al* 1987).

3. Results and discussion

3.1 Growth rate

Table 1 shows the growth rate of the coral, which varies from $\sim 6\text{mm y}^{-1}$ in the early stages to $\sim 3\text{mm y}^{-1}$ during the late stages, with an overall mean growth rate of 3.5mm y^{-1} . Because of the

Table 1. Growth rate, oxygen and carbon isotope ratios in the coral. Underlined data indicate the minimum values in carbon and oxygen isotope ratios. If adjacent data points are indistinguishable within the analytical uncertainty ($\pm 0.07\%$), the minima in $\delta^{18}\text{O}$ are chosen to correspond with $\delta^{13}\text{C}$ minima. $\delta^{18}\text{O}$ and $\delta^{13}\text{C}$ are relative to V-PDB standard.

Year (A.D.)	Distance (mm)	$\delta^{18}\text{O}$ (‰)	$\delta^{13}\text{C}$ (‰)	Growth rate (mm y^{-1})	Rain (mm)	$\delta^{18}\text{O}$ range (‰)
1948	0.0	-4.08	-0.54	5.4	201	0.37
	1.7	<u>-4.15</u>	<u>-1.12</u>			
	3.3	-3.78	-0.36			
	4.4	-3.86	-0.44			
1949	5.4	-3.73	-0.71	8.3	536	0.69
	6.3	-4.27	-1.82			
	7.5	<u>-4.37</u>	<u>-2.14</u>			
	8.4	-4.36	-1.54			
	9.5	-4.42	-1.14			
	10.7	-4.25	-0.72			
	11.8	-3.82	-0.50			
12.7	-3.84	-0.30				
1950	13.7	-3.69	-0.35	6.9	554	0.59
	15.4	-3.99	-0.22			
	17.0	-4.04	-0.23			
	18.8	<u>-4.28</u>	<u>-0.55</u>			
1951	20.6	-3.65	1.02	7.1	303	0.32
	22.6	-3.70	-0.09			
	24.5	-3.80	<u>-0.43</u>			
	26.2	<u>-3.97</u>	<u>-0.29</u>			
1952	27.8	-3.88	-0.20	4.2	392	0.52
	29.2	<u>-4.36</u>	<u>-1.72</u>			
	30.5	-4.40	-0.94			
1953	32.0	-4.10	-0.03	8.2	659	0.47
	34.0	-4.16	-0.99			
	35.0	<u>-4.57</u>	<u>-1.41</u>			
	36.3	-4.48	-1.41			
	38.6	-4.25	-0.54			
1954	40.2	-4.23	-0.26	3.8	526	0.45
	41.6	-4.68	-2.23			
	42.7	<u>-4.65</u>	<u>-2.52</u>			
1955	44.0	-4.20	-0.41	7.8	343	0.30
	45.7	-3.94	0.48			
	49.6	-4.23	-0.34			
	48.2	-4.24	-0.37			
	49.9	<u>-4.22</u>	<u>-0.81</u>			
	50.7	-4.03	-0.04			
1956	51.8	-3.99	0.02	3.5	710	0.20
	52.5	-4.07	-0.57			
	53.0	<u>-4.19</u>	<u>-0.56</u>			
	54.0	-4.07	-0.58			
1957	55.3	-3.75	<u>-0.59</u>	5.7	486	0.41
	57.2	-4.06	0.62			
	58.8	<u>-4.16</u>	0.35			
1958	61.0	-3.91	0.65	7.5	541	0.38
	62.5	-4.10	-0.05			
	63.8	-4.19	-0.42			
	65.1	<u>-4.29</u>	<u>-0.57</u>			
	66.6	-4.11	-0.26			
1959	68.5	-4.10	0.27	3.5	1241	0.43
	70.5	<u>-4.53</u>	<u>-0.58</u>			
1960	72.0	-4.25	0.00	5.1	290	0.29
	73.8	<u>-4.54</u>	<u>-1.34</u>			
	75.6	-4.42	-1.01			
1961	77.1	-4.27	0.04	5.2	785	0.07
	78.8	<u>-4.29</u>	<u>-0.77</u>			
	80.3	-4.22	-0.46			

(Continued)

Table 1. (Continued)

Year (A.D.)	Distance (mm)	$\delta^{18}\text{O}$ (‰)	$\delta^{13}\text{C}$ (‰)	Growth rate (mm y ⁻¹)	Rain (mm)	$\delta^{18}\text{O}$ range (‰)
1962	82.3	-3.98	-0.31	6.7	382	0.45
	83.9	<u>-4.40</u>	-0.26			
	85.6	<u>-4.23</u>	<u>-0.45</u>			
	87.5	-3.95	0.13			
1963	89.0	-3.73	0.12	5.0	351	0.43
	90.8	<u>-4.08</u>	<u>-0.66</u>			
	92.4	<u>-4.16</u>	<u>-0.39</u>			
1964	94.0	-3.85	0.54	6.4	491	0.15
	95.5	-3.90	-0.09			
	96.9	<u>-4.00</u>	<u>-0.81</u>			
	98.6	-3.98	-0.27			
1965	100.4	-3.70	0.19	3.0	415	0.47
	102.1	<u>-4.17</u>	<u>-0.98</u>			
1966	103.4	-3.92	-0.42	6.6	304	0.36
	105.2	-4.09	-0.03			
	106.7	-4.28	-0.15			
	108.2	<u>-4.20</u>	<u>-0.56</u>			
1967	110.0	-3.98	0.53	3.5	737	0.36
	111.9	<u>-4.34</u>	<u>-0.03</u>			
1968	113.5	-3.82	<u>-0.88</u>	3.3	319	0.12
	115.0	<u>-3.94</u>	0.94			
1969	116.8	-3.99	0.40	5.1	268	0.11
	118.2	-4.10	-0.06			
	120.2	<u>-4.01</u>	<u>-0.34</u>			
1970	121.9	-3.67	0.19	6.3	813	0.55
	123.8	<u>-4.22</u>	<u>-0.46</u>			
	125.5	-4.00	-0.50			
1971	128.2	-3.51	<u>-0.41</u>	4.6	418	0.23
	131.0	<u>-3.74</u>	-0.13			
1972	132.8	-3.65	0.05	4.3	212	0.19
	135.0	<u>-3.84</u>	0.22			
1973	137.1	-3.44	0.36	3.7	377	0.40
	139.2	<u>-3.84</u>	<u>-0.02</u>			
1974	140.8	-3.70	0.34	3.6	140	0.32
	142.7	<u>-4.02</u>	<u>-0.30</u>			
1975	144.4	-3.78	0.65	6.2	569	0.71
	145.8	-3.85	1.05			
	147.4	-4.24	<u>-0.14</u>			
	149.0	<u>-4.49</u>	<u>-0.10</u>			
1976	150.6	-4.35	0.32	3.8	520	0.10
	152.0	-4.43	-0.21			
	153.1	<u>-4.45</u>	<u>-0.48</u>			
1977	154.4	-4.30	0.21	5.6	529	0.26
	156.0	-4.41	0.06			
	157.2	<u>-4.54</u>	<u>-0.47</u>			
	158.8	-4.56	-0.22			
1978	160.0	-4.15	0.20	5.7	473	0.47
	161.5	-4.57	-0.01			
	162.9	<u>-4.62</u>	<u>-1.10</u>			
	164.3	-4.34	0.26			
1979	165.7	-4.28	0.52	4.3	974	0.70
	166.9	-4.94	-0.72			
	168.4	<u>-4.98</u>	<u>-0.73</u>			

(Continued)

Table 1. (Continued)

Year (A.D.)	Distance (mm)	$\delta^{18}\text{O}$ (‰)	$\delta^{13}\text{C}$ (‰)	Growth rate (mm y^{-1})	Rain (mm)	$\delta^{18}\text{O}$ range (‰)
1980	170.0	<u>-4.41</u>	<u>-0.28</u>	2.8	629	0.02
	171.5	-4.39	-0.24			
1981	172.8	-4.08	0.07	4.4	631	0.39
	174.4	<u>-4.47</u>	<u>-0.76</u>			
	175.6	-4.26	-0.37			
1982	177.2	-3.96	-0.06	2.2	365	0.18
	178.3	<u>-4.14</u>	<u>-0.26</u>			
1983	179.4	-3.96	0.57	4.7	626	0.17
	181.2	-4.03	-0.06			
	182.9	<u>-4.13</u>	<u>-0.29</u>			
1984	184.1	-3.69	0.65	4.4	388	0.19
	185.6	<u>-3.76</u>	<u>0.09</u>			
	187.3	-3.88	0.84			
1985	188.5	-3.77	0.75	2.5	268	0.17
	189.8	<u>-3.94</u>	<u>0.61</u>			
1986	191.0	-3.63	1.16	4.2	219	0.30
	192.8	-3.93	0.76			
	193.9	<u>-3.93</u>	<u>0.18</u>			
1987	195.2	-3.71	0.80	4.6	71	0.29
	196.4	-3.88	0.88			
	198.6	<u>-4.00</u>	<u>-0.02</u>			
1988	199.8	-3.74	0.77	6.1	718	0.47
	201.7	-3.85	0.49			
	203.9	<u>-4.21</u>	<u>0.00</u>			
1989	205.9	-3.90	<u>0.96</u>	3.1	529	0.19
	208.0	<u>-4.09</u>	1.57			

varying growth rate the number of subsamples per band for isotopic analyses also varied from 8 to 2. On an average about 7 sub-samples were taken from 2 annual bands. The sub-samples filed out had a finite width of ~ 1 mm, which could represent a time period of ~ 25 days in the best case (8 sub-samples per band) to ~ 3 months in the worst case (2 samples per band); it must be noted that ~ 1 to 2 mm gap was maintained between consecutive samples to avoid cross-contamination between them.

3.2 Oxygen isotopes

The oxygen ($\delta^{18}\text{O}$) and carbon ($\delta^{13}\text{C}$) isotopic data from annual bands of the coral sample are presented in figure 3(a and b). It is known that the $\delta^{18}\text{O}$ of biogenic marine CaCO_3 is determined by temperature and $\delta^{18}\text{O}$ of the water in which it grows (Shackleton 1967). Often, the $\delta^{18}\text{O}$ data for the sea water are not available and salinity can be used as a substitute, as the two are in general correlated (Craig and Gordon 1965). However, this relationship differs from region to region. COADS (Comprehensive Ocean Atmospheric Data Set) SST data (Sadler *et al* 1987) at 22.5°N , 70°E averaged over the past eighty years are shown in figure 2. The curve shows maximum SST (29°C) around June and minimum (23°C) around January–

February. A small trough during August–October shows a decrease in SST (2°C) probably because of cloud cover. An increase in SST would result in a decreased $\delta^{18}\text{O}$ value of the coral, as the temperature dependence of the fractionation factor is negative ($-0.24\text{‰ }^\circ\text{C}^{-1}$ for the species under consideration, Weber and Woodhead 1972). Therefore we infer that coral $\delta^{18}\text{O}$ maximum must occur in January and minimum in June, with a seasonal range of $\sim 1.44\text{‰}$ corresponding to the temperature range of 6°C . However, this has to be corrected for the $\delta^{18}\text{O}$ variations in sea water. We have also collected sea water samples from the coral location periodically and measured their $\delta^{18}\text{O}$ values (table 2). The mean winter (December to February) value is 0.68‰ while the mean summer (May–June) value is 0.92‰ (values relative to V-SMOW). Eventhough these values are the same within analytical precision ($\pm 0.15\text{‰}$), there appears to be a tendency towards higher $\delta^{18}\text{O}$ values during summer due to higher SST and consequent evaporation. Therefore we subtract $\sim 0.3\text{‰}$ from the calculated range of 1.44‰ . Thus the expected seasonal range in coral $\delta^{18}\text{O}$ is $\sim 1.1 \pm 0.15\text{‰}$. The observed mean seasonal $\delta^{18}\text{O}$ amplitude is $0.34 \pm 0.17\text{‰}$, as calculated from the data shown in table 1. The apparent discrepancy between the observed and calculated $\delta^{18}\text{O}$ amplitudes has been noted earlier by others

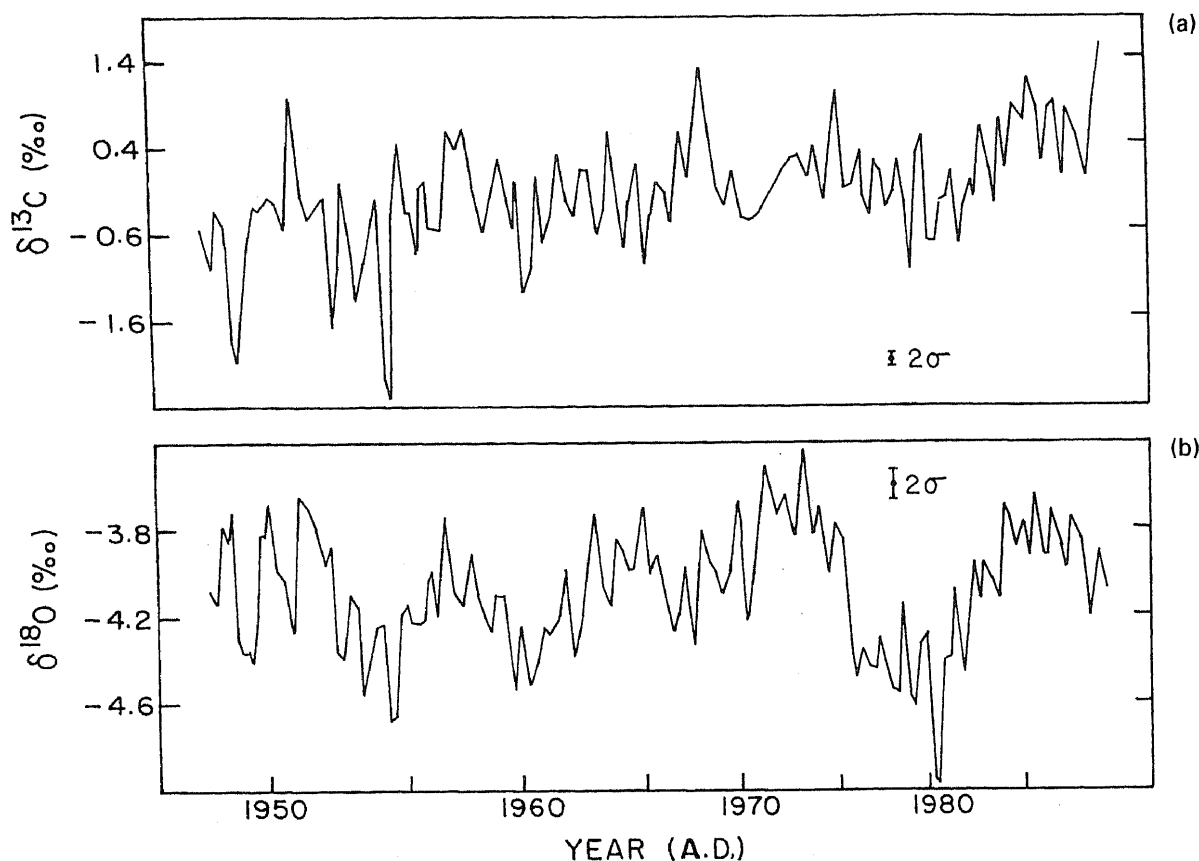


Figure 3. Carbon (a) and oxygen (b) isotopic records of the coral (*Favia speciosa*) for the period 1949-89 A.D.

Table 2. $\delta^{18}\text{O}$ of sea water (relative to V-SMOW standard) from the Gulf of Kutch.

Date of collection	$\delta^{18}\text{OSMOW}$ (‰)
24.11.92	0.75
21.12.92	0.61
18.01.93	0.76
17.02.93	0.63
05.05.93	0.93
10.06.93	0.91

Analytical uncertainty $\pm 0.15\%$.

(Emiliani *et al* 1978; Fairbanks and Dodge 1979; Leder *et al* 1991) and is explained in the present paper based on a model simulation, discussed in section 3.5.

3.3 Correlation with rainfall

Figure 4(a, b and c) respectively show annual minima in $\delta^{18}\text{O}$ and $\delta^{13}\text{C}$ of the coral (data underlined in table 1) and the monsoon (July to September) rainfall of Kutch and Saurashtra region for the period 1949-89 A.D. (India Meteorological Department's Records). Each annual minimum in $\delta^{18}\text{O}$ corresponds to June of that year, as explained in section 3.2. It can be seen that there is a negative correlation between $\delta^{18}\text{O}$ minima ($\delta^{18}\text{O}_m$, corresponding to the highest SST in the Gulf before commencement of the monsoon rains in Kutch) and the monsoon rainfall (figure 5). The

relationship between coral $\delta^{18}\text{O}$ and rainfall is given by:

$$\delta^{18}\text{O}_m = -3.906 - 6.498 \times 10^{-4} R$$

where R represents rainfall in mm. The correlation coefficient (r) is -0.56 ($n = 41$) significant at 0.01 level (P). In order to produce a change of 0.1‰ (detection limit) in coral $\delta^{18}\text{O}$ the rainfall has to change by ~ 150 mm. The magnitude of year to year variation in rainfall is ~ 340 mm (one standard deviation, calculated from data shown in table 1). This will cause a mean interannual change in the coral $\delta^{18}\text{O}$ of a magnitude 0.22‰. However, the difference in rainfall between two consecutive years can be as large as -700 to $+950$ mm, as seen from the rainfall record for the period 1949-89 A.D. (table 1); therefore the change in coral $\delta^{18}\text{O}$ can be as large as $+0.46$ to -0.63% . Figure 3(b) shows that such variations are indeed observed during some years when the sampling resolution is high.

In addition, there is a long term cycle of 7- to 8-year period that can be discerned visually from figure 3(b). [Power spectral analysis is not carried out because of (a) non-uniform sampling interval and (b) standard FFT codes either interpolate the data or fill with zeroes, which might produce spurious spectra, especially when the sampling resolution is coarse, forced by the slow growth rate of the coral]. This could be

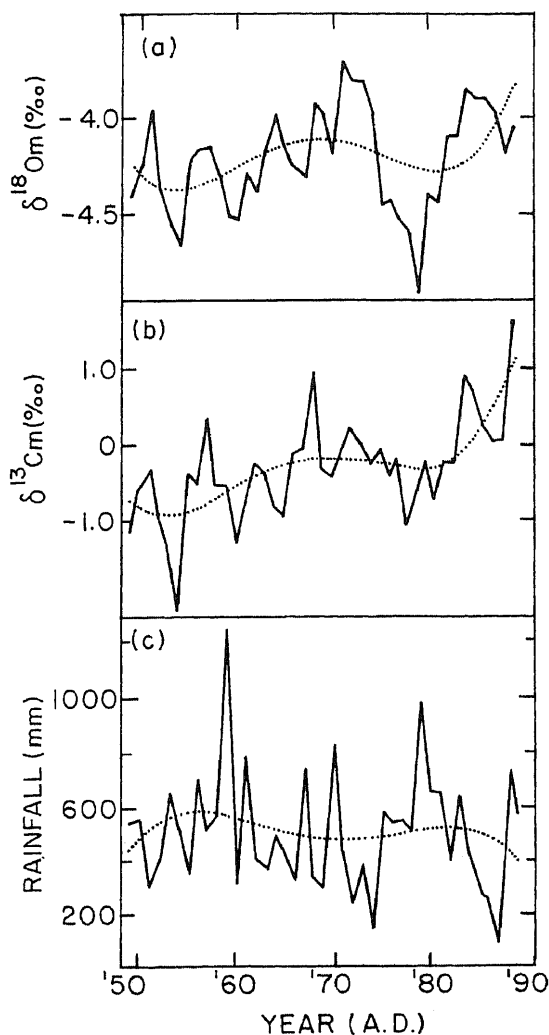


Figure 4. $\delta^{18}\text{O}$ minima (a), $\delta^{13}\text{C}$ minima (b) and monsoon rainfall (c) of the Kutch and Saurashtra region. The dotted curves are fourth order polynomials fitted to the data and indicate the long term trends.

due to a number of years of consistently increasing or decreasing rainfall. The consistently higher than normal rainfall during the late 70s is reflected as a dip in the coral $\delta^{18}\text{O}$ (figure 3b).

The dotted lines in figure 4(a, b and c) are fourth order regression lines through the data representing the trends. We used the trend lines to generate points of $\delta^{18}\text{O}$ and rainfall and found them to be correlated better: $r = -0.8$ ($n = 41$). This shows that while the long term changes in coral $\delta^{18}\text{O}$ can be used as a monsoon rainfall signal, seasonal variations tend to introduce noise in this signal. If the seasonal changes are removed by taking the average $\delta^{18}\text{O}$ of each year, this mean annual $\delta^{18}\text{O}$ is also found to be significantly correlated with monsoon rainfall over Kutch and Saurashtra ($r = -0.48$, $P < 0.01$). This observation is consistent with the theory of Shukla (1975) and observations of Shukla and Misra (1977) that the increase in SST in the Arabian Sea enhances the evaporation rate and hence the precipitation over Gujarat.

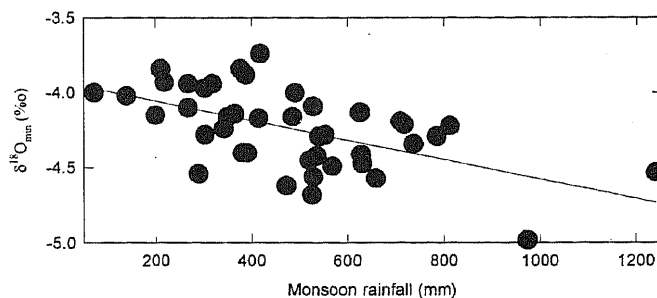


Figure 5. Correlation between monsoon rainfall and minima in $\delta^{18}\text{O}$.

3.4 Carbon isotopes

The $\delta^{13}\text{C}$ values show a long term increase of about 2‰ during the forty years of the coral growth, from a mean of ~ -1 ‰ during the early stages to the present day mean value of 1‰ (figure 3a). The cause of this long term trend is not clear. Growth rate related ^{13}C fractionation may be a likely cause, as suggested by McConnaughey (1989). In the earlier stages of growth, the mean growth rate is higher ($\sim 6 \text{ mm y}^{-1}$) whereas in the later stages, the mean growth rate is between 3 and 4 mm y^{-1} . This would contribute to the relative enrichment of ^{13}C during the later stages (figure 6). It is currently not possible to estimate the expected ^{13}C enrichment, as experimental data on photosynthesis rates of coral zooxanthellae and consequent ^{13}C enrichment are not available for any type of corals from the Arabian Sea region.

Like $\delta^{18}\text{O}$, $\delta^{13}\text{C}$ also shows annual oscillations with an average amplitude of about 1‰ (figure 3a). The minimum in $\delta^{13}\text{C}$ occurs during June–July, approximately at the same time when the minimum in $\delta^{18}\text{O}$ occurs, as can be seen from table 1. In fact, $\delta^{18}\text{O}$ and $\delta^{13}\text{C}$ are significantly positively correlated ($r = 0.56$). The reason for the minimum in $\delta^{13}\text{C}$ during June–July is probably the reduced rate of photosynthesis during this time of the year compared to the pre-monsoon (February to May) and post-monsoon (October to January) seasons. As is well known, photosynthesis discriminates against ^{13}C and makes the marine bicarbonate enriched in ^{13}C in seasons of high phytoplankton photosynthetic activity (McConnaughey 1989). Qasim (1982) has observed that, in general, the phytoplankton productivity is high in the Indian coastal regions of the northern Arabian Sea. The average surface productivity for this region is 18.86, 7.0 and $25.12 \text{ gC m}^{-2} \text{ day}^{-1}$ for the pre-monsoon (March to May), monsoon (June to September) and post-monsoon months (November to January) respectively (table 8 of Qasim 1982). In addition, Madhupratap *et al* (1996) made a comprehensive set of measurements in the north eastern Arabian Sea, which indicate that winter (February) productivity ($807 \text{ mgC m}^{-2} \text{ d}^{-1}$) was higher than that during April–May ($310 \text{ mgC m}^{-2} \text{ d}^{-1}$) in the upper 120 m, near the

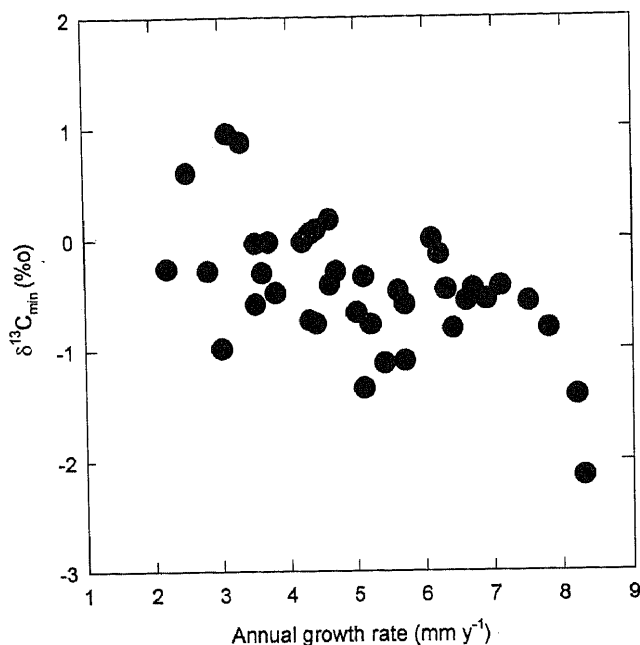


Figure 6. Correlation between coral growth rate and minima in $\delta^{13}\text{C}$.

Gulf of Kutch. The lowest biological productivity during the monsoon period, probably leads to the depletion of ^{13}C in the coral. A possible reason for the lower productivity during the monsoon season may be the cloud cover over the region, cutting off sun light. According to Fairbanks and Dodge (1979), reduced light intensity due to cloudiness reduces the coral $\delta^{13}\text{C}$.

3.5 Effect of sampling on the retrieval of the climatic signal

The retrieval of climatic information from the isotopic profiles of corals depends largely on the sampling resolution. Early attempts to link the coral $\delta^{18}\text{O}$ records to SST were not successful as observed by Goreau (1977) and Emiliani *et al* (1978). This apparent drawback of isotopic study was attributed to the sampling resolution problem by Fairbanks and Dodge (1979). They showed that with the analysis of as much as twelve sub-samples per annual band, they were able to recover the full seasonal amplitude of SST from the coral $\delta^{18}\text{O}$ measurements. The lesser the number of sub-samples per annual band, the greater the chances of missing the maxima and minima in the coral $\delta^{18}\text{O}$. Moreover, in the case of very narrow annual bands, it is difficult to get more than a few sub-samples per band for isotopic analyses. Furthermore, a sub-sample taken by filing or drilling has a finite width (say ~ 1 mm), which, in the case of a narrow band, can average the SST signal for a period of as much as six months. Thus depending on the coral growth rate (i.e., the skeletal extension rate) and the sampling interval, the measured seasonal $\delta^{18}\text{O}$ amplitude can be greatly

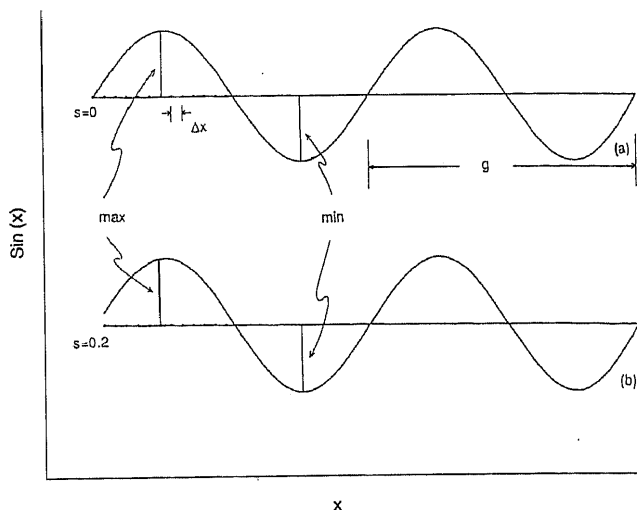


Figure 7. Illustration of sub-sampling the seasonal climatic signal; s is the distance from the origin of the first sample (phase). (a) $s = 0$, i.e., phase = 0 and (b) $s = 0.2$, or phase = 7.2° . Δx is the sampling interval and g stands for annual growth increment.

reduced compared to its actual value. To assess the magnitude of this reduction, we performed a simple computer simulation.

Since the annual $\delta^{18}\text{O}$ variations in a coral can be idealized, in the zeroth order approximation, to sinusoidal variations, we generated twenty cycles of a sine wave of unit amplitude and a (spatial) period of 10 mm. This would correspond to a $\delta^{18}\text{O}$ time series of a coral having a twenty year growth with an annual growth increment (g) of 10 mm. Implicit in our use of unit amplitude throughout the twenty cycles is that the seasonality in climate forcing did not change during this period (i.e., interannual variability is zero). Also the constant spatial period represents a uniform annual growth increment throughout the twenty years of the coral life span. We sub-sample this time series for different constant sub-sampling intervals ($\Delta x = 1, 2, 3, 4$ and 5 mm) and consider each sub-sample as a datum point. The maxima and minima in this sampled time series are identified (figure 7). The sum of the magnitudes of the maximum and minimum in each cycle is divided by two to obtain the mean amplitude for each cycle. Then the average of these mean amplitudes of the twenty cycles is calculated and is termed as the 'retrieved amplitude'. We establish a functional relationship between $\Delta x/g$ (reciprocal of the number of sub-samples per band) and A (the ratio of the retrieved amplitude to the actual amplitude). Obviously $A \leq 1$, because the sampling process tends to reduce the signal and at best can retrieve the actual amplitude. In practice, when the coral is collected, the annual cycle corresponding to the year of collection may not be complete. Hence the sampling may not commence at phase = 0 of the sine wave. Therefore the above exercise was repeated for different values of (a) s , the starting

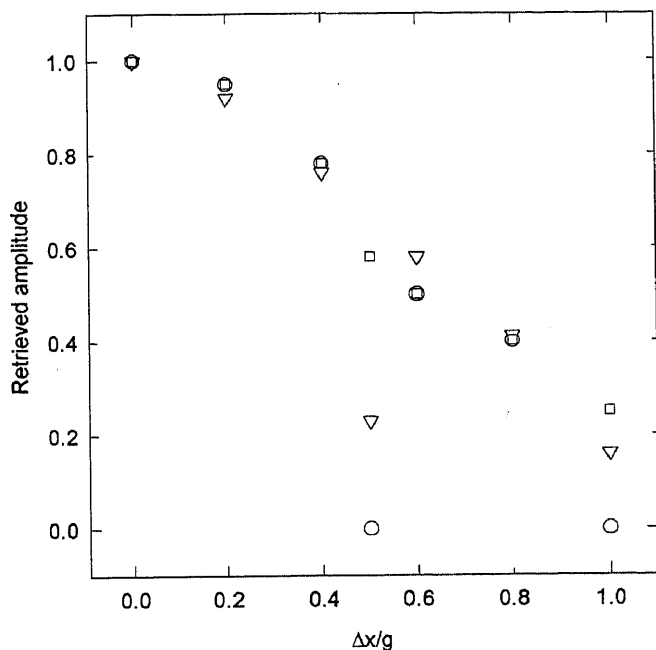


Figure 8. Variation of A (ratio of the retrieved amplitude to the true amplitude) as a function of $\Delta x/g$ [ratio of sampling interval to the constant (5 mm) annual growth increment]. Different symbols indicate different starting distances from the origin (s): Open circle $s = 0$; inverted triangle, $s = 0.2$; square, $s = 0.5$.

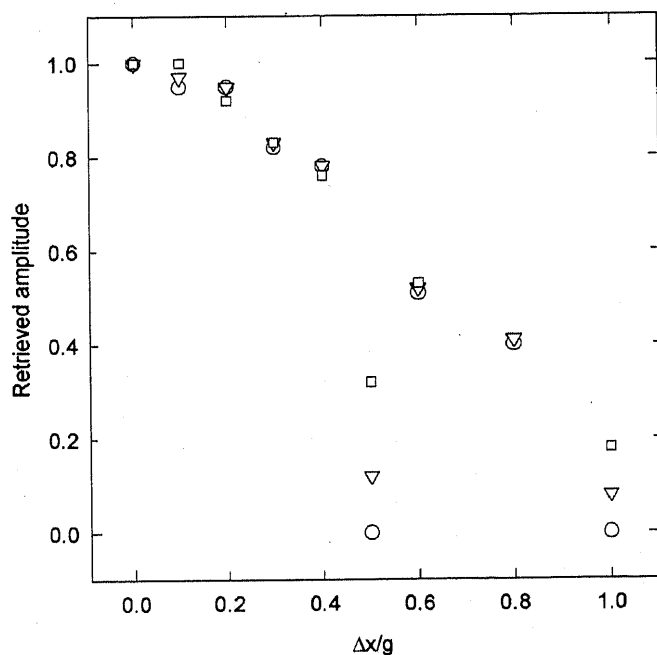


Figure 9. Same as figure 6, but for a constant growth increment (g) of 10 mm.

distance of the first sub-sampling point (i.e., different phases) and (b) g (but kept constant throughout the twenty year span, spatial periods of 5 and 10 mm).

Figures 8 and 9 show plots of A versus $\Delta x/g$ when $g = 5$ and 10 mm respectively. Circles denote the values of A for cases when $s = 0$ (sampling started with zero phase) and inverted triangles and squares

denote cases when the sampling started at phases of 14.4° and 36° ($s = 0.2$ and 0.5 mm from the origin) respectively.

It is obvious that when $\Delta x/g = 0$ (i.e., infinitely close sampling), we retrieve the full amplitude (i.e., $A = 1$) and when $\Delta x/g = 0.5$ or 1 (sampling interval = half or full spatial period), $A = 0$, if the sampling starts at origin (i.e., zero phase). This is seen in figures 8 and 9. For the rest of the values of $\Delta x/g$, A lies between 0 and 1. As $\Delta x/g$ increases, there is a general reduction in A . For example, when $\Delta x/g = 0.8$, 60% of the amplitude is lost. For the other cases when the sampling started with non-zero phase, the general trend is the same. However, for $\Delta x/g = 0.5$, we do get A values above zero. This is because the sample points do not lie on the zeroes of the sine curve, but slightly off the zeroes, providing some 'amplitude'. Further as the phase increases from 0 to 36° , the scatter in A increases around $\Delta x/g = 0.5$ and 1. The higher the starting phase, the higher is the retrieved amplitude (at these two abscissae). If a reduction of 10% in the amplitude is acceptable, then $\Delta x/g$ must be at least ~ 0.3 , i.e., approximately a minimum of four sub-samples per annual band.

In another simulation (a first order approximation), we assumed that while there is no interannual climatic variability, the annual growth increment varies in a random fashion between 2.5 to 5 mm (similar to the growth rate variation in the Gulf of Kutch (GK) coral; growth rate varies due to, say, changes in nutrient supply). Since a simple sine function has a constant (spatial) period, a variable growth rate cannot be represented by such a function. To circumvent this, we generated single cycles of twenty sine functions of unit amplitude but with varying periods (2.5 to 5 mm). Then we made the composite function by putting the sine function in the same time sequence as their growth rates in the case of the GK coral. The end points of the cycles match because the value of the sine functions in a full cycle is zero at either end ($0, 2\pi$). This curve is then sampled as before to obtain A for different Δx (1, 2, 3 and 4 mm) and s ($0^\circ, 18^\circ$ and 45°) values. In this case $\Delta x/g$ is not a constant as g varies with time. Therefore we plot A versus $\Delta x/g$ where g is the average of all g 's (~ 4 mm). Figure 10 shows the results; the reduction in amplitude is more or less the same as in the earlier case of constant growth increments. For example, for $\Delta x/g = 0.2$, A is 0.92 ± 0.07 , the same within the uncertainty as 0.95 for $\Delta x/g = 0.2$ (constant g). However a direct comparison is made difficult by the observation that even for the case when the sampling is done with zero phase, A is not zero for $\Delta x/g = 0.5$ and 1. This is understandable because the annual growth increment is varying and therefore even for $s = 0$, some amplitude is recovered for $\Delta x/g = 0.5$ and 1.

In addition to the sampling interval, another factor which reduces the retrieved amplitude is the

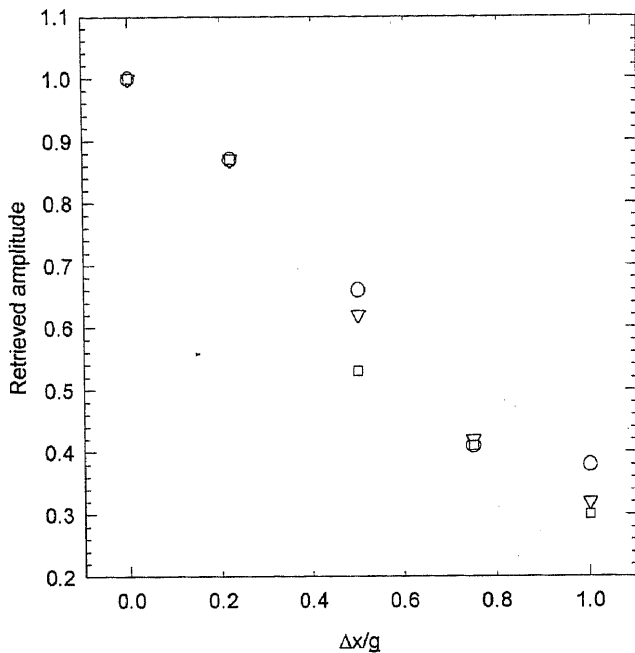


Figure 10. Same as figure 6, but for a variable growth increment ($g = 2.5$ to 5 mm).

averaging of the signal due to finite sub-sample thickness. We considered the effect of sampling thickness on the amplitude in the following way (second order approximation): we sampled the data generated for the variable growth increment case at different intervals, but now by averaging 1 mm around each sample. For this case the reduction in amplitude was found to be 40% for a $\Delta x/g$ value of 0.38, very similar to the value of $\Delta x/g$ in the GK coral. Using this we can compute the approximate magnitude of the actual seasonal $\delta^{18}\text{O}$ amplitude in the GK coral. The observed amplitude of $0.34 \pm 0.17\text{‰}$ can be considered to be 60% of the actual amplitude, therefore the actual amplitude would be $0.57 \pm 0.28\text{‰}$. This is about a factor of two less than the calculated amplitude of $1.1 \pm 0.15\text{‰}$. Considering the uncertainty in these estimates, it can be argued that the expected and observed $\delta^{18}\text{O}$ amplitudes are consistent within $\pm 2\sigma$ uncertainties. However, they could be genuinely different for reasons other than those considered above. These include: (i) The model does not consider year to year changes in $\delta^{18}\text{O}$ of sea water that may be caused by fresh water input (rainfall or run-off due to minor discharges from seasonal streams). (ii) The calculated coral $\delta^{18}\text{O}$ amplitude may be an over estimate as (a) the temperature coefficient for our sample may be different from that of the coral for which the value is reported by Weber and Woodhead (1972); we have used their value as this is the only available value in the literature for the genus *Favia*. However, there may be variations from species to species and from place to place. For instance McConnaughey (1989) reported temperature coeffi-

cients of 0.205 and 0.015 for *Pavona clavus* samples, one from Champion Island and the other from Punta Pitt, separated by 100 km; (b) we do not have the SST data in the exact location of the coral. The actual variations in SST may not be identical to what we have assumed. Further, the data (Sadler *et al* 1987) used by us is averaged over eighty years and does not contain any information on the year-to-year variability. The data were read off from contours spaced at 1°C intervals. In general, these data are compiled from records of ships that passed through the region. Whereas for the Pacific and Atlantic, there are more than 100 ship records, for the Indian Ocean there are only twenty five ship records. This may even be less for the Gulf of Kutch.

Notwithstanding the above possible uncertainties, we get a reasonably good agreement between the calculated and observed $\delta^{18}\text{O}$ amplitudes.

4. Conclusions

Coral $\delta^{18}\text{O}$ and summer monsoon rainfall are correlated, which can be used for qualitative reconstruction of historical rainfall records and also help understand the role of the Arabian SST in determining the inter-annual variability of monsoon rainfall over India. It is necessary that a very close sampling is done for the $\delta^{18}\text{O}$ analysis in order to retrieve the full seasonal cycle. The $\delta^{13}\text{C}$ variations in these corals could be used to substantiate past productivity/monsoon reconstructions, since they appear to be mainly controlled by cloudiness.

Acknowledgements

We thank M Bhaskaran and colleagues at CMFRI, Sika for assistance in sample collection; Ravi Bhushan, D N Yadav and R A Jani for help; M I Patel for guidance; S Krishnaswami and G B Pant for useful suggestions and encouragement. We thank referees P K Swart, S K Bhattacharya, M S Srinivasan and Rupa Kumar Kolli for comments and suggestions to improve the manuscript. This project was funded by the ID-GBP and partly by INSA.

References

- Aharon P 1991 Recorders of reef environment histories: Stable isotopes in corals, giant clams, and calcareous algae; *Coral Reefs* 10 71–90
- Chakraborty S and Ramesh R 1992 Climatic significance of $\delta^{18}\text{O}$ and $\delta^{13}\text{C}$ variations in a banded coral (*Porites*) from Kavaratti, Lakshadweep islands; In, *Oceanography of the Indian Ocean* (ed) B N Desai (New Delhi: Oxford & IBH) pp. 473–478
- Chakraborty S and Ramesh R 1993 Monsoon induced sea surface temperature changes recorded in Indian corals; *Terra Nova* 5 545–551

- Chakraborty S and Ramesh R 1997 Environmental significance of carbon and oxygen isotope ratios of banded corals from Lakshadweep, India; *Quaternary International* **37** 55–65
- Charles C D, Hunter D E, Fairbanks R G 1997 Interaction between the ENSO and the Asian monsoon in a coral record of tropical climate; *Science* **277** 925–928
- Cole J and Fairbanks R G 1990 The southern oscillation recorded in the $\delta^{18}\text{O}$ of corals from Tarawa atoll; *Paleoceanography* **5** 669–683
- Craig H and Gordon L 1965 Deuterium and oxygen-18 variation in the ocean and the marine atmosphere; In *Stable isotopes in Oceanographic Studies and Paleotemperatures* (ed) E Tongiorgi (Spoleto) pp. 9–130
- Druffel E M 1985 Detection of El Niño and decade time scale time variability of sea surface temperature from banded coral records: Implications for the carbon dioxide cycle; In *The carbon cycle and atmospheric CO₂ natural variations Archean to Present* (eds) E T Sundquist and W S Broecker, Geophysical Monograph **32** (Washington DC: American Geophysical Union) pp. 111–112
- Dunbar R B and Wellington G M 1981 Stable isotopes in a branching coral monitor seasonal temperature variation; *Nature* **293** 453–455
- Emiliani C, Hudson J H, Shinn E A and George R Y 1978 Oxygen and carbon isotopic growth records in a reef coral from the Florida Keys and a deep sea coral from Blake Plateau; *Science* **202** 627–629
- Fairbanks R G and Dodge R E 1979 Annual periodicity of the $^{18}\text{O}/^{16}\text{O}$ and $^{13}\text{C}/^{12}\text{C}$ ratios in the coral *Montastrea annularis*; *Geochim. Cosmochim. Acta* **43** 1009–1020
- Goreau T J 1977 Coral skeleton chemistry: Physiological and environmental regulation of stable isotopes and trace metals *Montastrea annularis*; *Proc. R. Soc. London* **B196** 291–315
- Leder J J, Szmant A M and Swart PK 1991 The effect of prolonged bleaching on skeletal banding and stable isotopic composition *Montastrea annualris*; *Coral Reefs* **10** 19–27
- Madhupratap M, Prasanna Kumar S, Bhattathiri P M A, Dileep Kumar M, Raghukumar S, Nair K K C and Ramaiah K (1996) Mechanisms of biological response to winter cooling in the northern Arabian Sea; *Nature* **384** 549–552
- McConnaughey T 1989 ^{13}C and ^{18}O isotopic disequilibrium in biological carbonates I: Patterns; *Geochim. Cosmochim. Acta* **53** 151–162
- Qasim S Z 1982 Oceanography of the Northern Arabian Sea; *Deep Sea Res.* **9** 1041–1068
- Sadler J C, Lander M A, Hori A M and Oda L K 1987 Tropical marine climate atlas 2 *Indian Ocean and Atlantic Ocean* (University of Hawaii Department of Meteorology)
- Shackleton N J 1967 Oxygen isotope analyses and Pleistocene temperatures reassessed; *Nature* **215** 43–46
- Shen G T and Sanford C L 1990 Trace element indicators of climatic variability in reef building corals; In *Global Ecological Consequences of the 1982–83 El Niño-Southern Oscillation* (ed) P W Glynn (New York: Elsevier) pp. 255–284
- Shetye S R, Gouveia A D, Shenoi S S C, Sundar S, Michael G S, Almeida A M and Santanam K 1990 Hydrographic and circulation off the west coast of India during the Southwest monsoon 1987; *J. Mar. Res.* **48** 359–378
- Shukla J 1975 Effect of Arabian Sea surface temperature anomaly on Indian summer monsoon: A numerical experiment with the GFDL model; *J. Atmos. Sci.* **32** 503–511
- Shukla J and Misra B N 1977 Relationship between sea surface temperature and wind speed over the central Arabian Sea and monsoon rainfall over India; *Mon. Weather. Rev.* **105** 998–1002
- Weber J N and Woodhead P M J 1972 Temperature dependence of oxygen-18 concentration in reef coral carbonates; *J. Geophys. Res.* **77** 463–473
- Wellington G M and Glynn P W 1983 Environmental influences on skeletal banding in eastern Pacific (Panama) corals; *Coral Reefs* **1** 215–222